

High energy neutrino yields from astrophysical sources I: Weakly magnetized sources

M . Kachelrie ¹ and R . Tom as²

¹Institutt for fysikk, NTNU Trondheim , N {7491 Trondheim , Norway

²AHEP Group, Institut de Física Corpuscular – C.S.I.C./Universitat de Valencia
 Edifici Instituts d’Investigacio, Apt. 22085, E-46071 Valencia, Spain

We calculate the yield of high energy neutrinos produced in astrophysical sources with negligible magnetic fields varying their interaction depth from nearly transparent to opaque. We take into account the scattering of secondaries on background photons as well as the direct production of neutrinos in decays of charm mesons. If multiple scattering of nucleons becomes important, the neutrino spectra from meson and muon decays are strongly modified with respect to transparent sources. Characteristic for neutrino sources containing photons as scattering targets is a strong energy-dependence of the ratio R^0 of ν_e and ν_μ fluxes at the sources, ranging from $R^0 = \nu_e/\nu_\mu = 0$ below threshold to $R^0 \approx 4$ close to the energy where the decay length of charged pions and kaons equals their interaction length on target photons. Above this energy, the neutrino flux is strongly suppressed and depends mainly on charm production.

PACS numbers: 95.85.Ry, 98.70.Sa, 14.60.Lm, 14.60.Pq,

I. INTRODUCTION

Experimental high energy neutrino physics has become one of the most active areas of astroparticle physics, offering among others the prospect of identifying the sources of ultra-high energy cosmic rays [1]. High energy neutrinos from astrophysical sources are the decay products of secondary mesons produced by scattered high energy protons on background protons or photons. The classic example are the so-called cosmogenic or GZK neutrinos produced in scatterings of extragalactic ultra-high energy cosmic rays on cosmic microwave photons during propagation [2]. Two different kind of bounds on high energy neutrino fluxes exist: The cascade or EGRET limit uses bounds on the diffuse MeV–GeV photon background to limit the energy transferred to electromagnetically interacting particles that are produced unavoidably together with neutrinos [3]. The cosmic ray upper bounds of, e.g., Refs. [4, 5] use the observed ultra-high energy cosmic ray flux to limit possible neutrino fluxes. The latter limit assumes that all neutrino sources are transparent to hadronic interactions and thus at least neutrons can escape from the source region without interactions. Dropping the assumption of transparent sources and hiding the acceleration region by sufficient material absorbing ultra-high energy cosmic rays allows one to avoid the cosmic ray limits. One might therefore speculate that large neutrino fluxes at high and ultra-high energies might be produced in opaque sources, as they are needed, e.g., to perform neutrino absorption spectroscopy [6].

In this work, we calculate the flux of high energy neutrinos produced as secondaries in astrophysical sources. We consider sources with interaction depth ranging from nearly transparent to opaque. In contrast to most earlier investigations [7, 8, 9], we put emphasis on sources with such high densities that magnetic fields can be neglected and multiple scatterings are important. As a result, the neutrino spectra from meson and muon decays are strongly modified with respect to transparent

sources. Since in most astrophysical environments the depth for pions is above threshold much larger than for pp interactions, we consider photons in the source as target material. In Sec. 2, we discuss the relevant production processes and present the neutrino yields from a single source. We discuss also briefly the consequences of the derived energy dependence of the neutrino yields on the expected high energy neutrino fluxes from astrophysical sources. In Sec. 3, we examine the neutrino flavor composition at the source as well as the effect of neutrino oscillations on the flavor composition at the detector and significant deviations from the canonical flavor ratio expected from pion decay. Finally, we summarize our results in Sec. 4.

II. NEUTRINO PRODUCTION PROCESSES AND YIELDS

A. Simulation and particle interactions

We idealize a hidden neutrino source as an homogeneous slab filled with photons in which high energy protons are injected. The probability N that a particle travels in the slab the distance L without scattering or decay is given by

$$N = \exp \left[-L \int_0^L \frac{dl}{(l_{i=2} + l_{int})} \right]; \quad (1)$$

where $l_{i=2}$ and l_{int} are its decay and interaction length, respectively. Their relative value determines the fate of the particle, either it decays or scatters.

In our Monte Carlo simulation, we track explicitly all secondaries (N ; ν ; K ; $K_{L,S}^0$) for which the interaction rate is non-negligible compared to their decay rate. We determine their multiplicity and energy spectra of light secondary particles produced in scattering processes with a modified version of SOPHIA [10]. For the case of hadrons

arXiv:astro-ph/0606406v1 16 Jun 2006

containing charm quarks, we employ HERWIG [11] to determine the differential energy spectra of prompt charm neutrinos, while we estimate the total cross section for charm production from Ref. [12]. To fix the pion-photon and kaon-photon interactions, we use the following simple recipe [13]: We determine first the maximum of the resonant production cross section in the Breit-Wigner approximation of ρ and K^* , respectively, and compare it to $p + \pi \rightarrow \rho + \pi$ and $p + \pi \rightarrow K^* + \pi$. Then we rescale the proton-photon cross section by the ratios of the maxima to obtain the pion-photon and kaon-photon cross sections in the non-resonant region. Finally, the interaction length l_{int} is calculated from

$$l_{\text{int}}^{-1} = \frac{1}{2} \int_{\epsilon_{\text{th}}}^{\epsilon} d\epsilon \frac{d\sigma_{\text{had}}(\epsilon)}{d\epsilon} \frac{1}{\epsilon^2}; \quad (2)$$

where γ is the Lorentz factor of the hadron in the lab frame, ϵ_{th} is the threshold energy of the relevant reaction in the rest system of the hadron, and $n(\epsilon)$ the energy distribution of photons with energy ϵ in the lab frame.

B. Phenomenological characterization of the sources

In the following, we do not consider any particular model of neutrino sources, but characterize instead the sources in a phenomenological way. This allows us to perform a systematic analysis of different sources according to their thickness, from nearly transparent ones where the accelerated protons hardly scatter once with the surrounding material to completely opaque sources where neither high energy cosmic rays nor high energy photons can escape. In our idealization of a neutrino source as an homogeneous slab filled with photons, each source is fully characterized by its length L and the photon distribution $n(\epsilon)$. Potential sources of photon backgrounds are manifold, but we restrict ourselves in this work to the most important example, a background of thermal photons at temperature T .

A more severe restriction of the current work is that we consider only sources with negligible magnetic fields. Thus we require that i) energy losses due to synchrotron losses are much smaller than due to interactions and that ii) deflections of charged particles in magnetic fields are small compared to the size of the source. This limitation allows us to stress more clearly the salient features of opaque sources. In a subsequent work, we shall consider the generic case of sources with arbitrary interaction depth and magnetic fields [14].

For the discussion of our numerical results it is useful to introduce following Ref. [7] several dimensionless quantities. The first one is the "interaction depth" of nucleons defined analogously to the optical depth as the ratio $\tau = L/l_{\text{int}}$ of the size L of the source to the interaction length l_{int} of nucleons. This ratio determines, if most of the protons leave the source without interactions ($\tau \ll 1$ or "transparent source"), or if multiple-scattering

of nucleons is important and mesons are efficiently produced ($\tau \gg 1$ or "opaque source"). For the illustration of our numerical results, we determine in the following via $l_{\text{int}}^{-1} = \int_{\epsilon_{\text{th}}}^{\epsilon} d\epsilon \frac{d\sigma_{\text{had}}(\epsilon)}{d\epsilon} \frac{1}{\epsilon^2}$ with $\sigma_{\text{had}} = 0.2$ mb as reference cross section.

As second parameter we introduce the dimensionless energy $x = E/\epsilon_p = \epsilon/\epsilon_p$, where $\epsilon = \gamma m_p$ denotes the energy of the maximum of the Planck distribution and m_p the proton mass. This parameter allows one to express the different yields in the form of a universal function, which in the case of transparent sources does not explicitly depend on the temperature. Finally, it is useful to introduce the critical dimensionless energy $x_{\text{cr}} = E_{\text{cr}}/\epsilon_p = \epsilon_{\text{cr}}/\epsilon_p$, where $E_{\text{cr}} = \epsilon_{\text{cr}} = \gamma m_p$ is defined as the energy at which the decay length $\lambda_{1=2} = c \tau_{1=2} = l_0$ of a meson with lifetime $\tau_{1=2}$ and mass m is equal to its interaction length l_{int} . Using charged pions as reference particles, x_{cr} depends numerically as $x_{\text{cr}} \approx 2 \cdot 10^0 = (T/K)^2$ on the temperature of thermal photons. Thus, the parameter determines the fraction of nucleons that scatter on photons, while the parameter x controls if mesons mainly decay ($x < x_{\text{cr}}$) or scatter ($x > x_{\text{cr}}$).

Before we discuss the details of the different spectra, we briefly comment on the main characteristics of hadron-photon interactions. In the upper panel of Fig. 1, we show the interaction length of protons, pions and kaons in a thermal bath of photons with temperature $T = 10^4$ K together with their decay length as function of the dimensionless energy x (bottom axis) or their energy (upper axis). The fate of a hadron is characterized by two important energies: The threshold energy at $x_{\text{th}} \approx 0.1$, below which photo-meson reactions are exponentially suppressed, and the critical energy x_{cr} , above which most mesons will scatter before decaying. If the decay length and the interaction length cross inside the source, $l_{1=2} = l_{\text{int}} < L$, the effect of multiple scattering has to be taken into account. Main consequence is a strong suppression of the high energy neutrino flux produced in meson decays for $x > x_{\text{cr}}$. The shorter lifetime of heavier mesons leads to a shift of their critical energy, i.e. $x_{\text{cr}}^K > x_{\text{cr}}^\pi$.

In the lower panel of Fig. 1, we show the interaction and decay length of hadrons as a function of x for sources with different temperature T . As expected from the temperature dependence of l_{int} and the definition of x , the critical energy x_{cr} does not only depend on the meson considered but also on the temperature: x_{cr} scales simply as $x_{\text{cr}} \propto 1/T^2$ as long as x_{cr} is above threshold, $x_{\text{cr}} > x_{\text{th}} \approx 0.1$. Thus, multiple scattering starts to become important at lower energies as the source temperature increases. On the other hand, the dimensionless threshold energy x_{th} is nearly independent of T . Therefore in the case of opaque sources the range with unsuppressed neutrino fluxes, $0.1 < x_{\text{th}} < x < x_{\text{cr}}/1=T^2$, shrinks for increasing T and becomes a narrow peak around x_{th} for $T > 5 \cdot 10^5$ K. On the other hand, large neutrino fluxes at energies high enough to perform neutrino spectroscopy, $E_{\text{cr}} > 10^{21}$, can be obtained only in

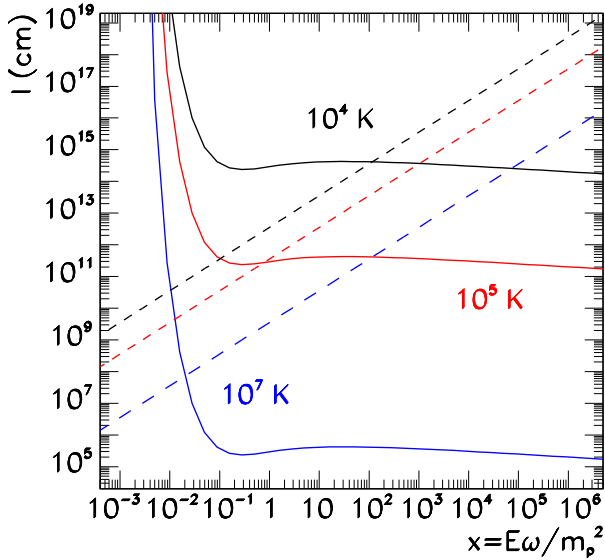
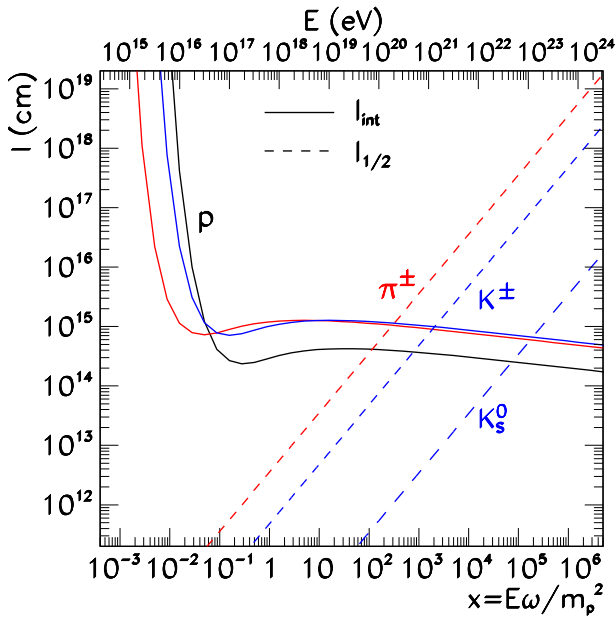


FIG. 1: Top: Interaction length (solid lines) for proton (black), charged pions (red) and charged kaons (blue) with thermal photons at a temperature $T = 10^4$ K, together with the decay length (dashed lines) for π^\pm , K^\pm and K_S^0 . Bottom: Interaction length (solid lines) for proton and decay length (dashed lines) of charged pions for sources at $T = 10^4$ K (black), $T = 10^5$ K (red), and $T = 10^7$ K (blue).

sources at low temperatures, $T < 5 \cdot 10^3$ K. If, additionally, one requires the source to be opaque so that the high-energy cosmic ray flux is suppressed, e.g. $\tau > 10$, then a second condition for a suitable source is a large extension, $L > 3 \cdot 10^{27} = (T=K)^3$ cm.

C. Neutrino yields and fluxes from a single source

In order to analyze the effect of the thickness of the source on the neutrino spectrum we study the neutrino yield of a single source. The neutrino yield $Y(E)$, i.e. the ratio $Y(E) = \Phi(E) / \Phi_p(E) = \langle n_\nu(E) \rangle$ of the emitted neutrino flux and the product of the depth and the injected proton flux Φ_p , represents the number of neutrinos produced per injected proton with the same energy. For the energy spectrum of the injected protons we assume a power law $dN = dE / E^\alpha$ with $\alpha = 2.2$, consistent with typical predictions for Fermi shock acceleration. For illustration we choose the maximal energy of the initial proton spectrum as $E_{\text{max}} = 10^{24}$ eV.

Let us first describe the different reactions contributing to the neutrino flux. In Fig. 2, we show the various contributions to Y for the case of an intermediate value of the interaction depth, $\tau = 0.4$ [22]. The low energy tail of neutrinos arises from the decay of neutrons, $n \rightarrow p + e + \bar{\nu}_e$, where the energy fraction transferred to neutrinos is on average only $\sim 10^{-3}$. At all other energies, charged pions are produced most efficiently and their decay products provide the dominating contribution to the neutrino yield. The various decay channels of kaons contribute around 10% to the neutrino yields. The neutrino yield from prompt decays of charm mesons is even smaller, because of the relative high mass of charm mesons resulting in a high energy threshold and small cross section for charm production.

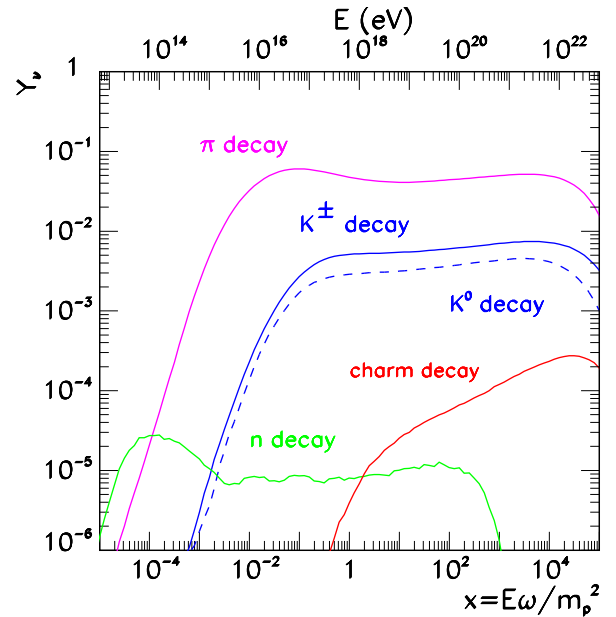


FIG. 2: Neutrino yield Y as function of $x = E \omega / m_p^2$ from the decay of π (magenta), K^\pm (solid blue), K^0 (dashed blue), neutrons (green), and charm mesons (red) for a source with $T = 10^4$ K and $\tau = 0.4$.

Next we discuss the effect of multiple scatterings on the different neutrino yields. In the top panel of Fig. 3,

we show the yields from meson decays for a source with $T = 10^4$ K and three different sizes, $L = 10^{13}$ cm ($\tau = 0.04$), 10^{14} cm ($\tau = 0.4$) and 10^{16} cm ($\tau = 40$), respectively. For $\tau < 1$, multiple scattering is negligible, $\tau > 1$ and the neutrino yields expressed as functions of x are thus independent from L . Moreover, the neutrino yield from charm meson decays is clearly subdominant. Increasing the size of the source, multiple scattering cannot be neglected anymore and three different x regions can be distinguished. For $x < x_{cr}$, most pions decay before scattering and, as in the case of transparent sources, the neutrino yield is dominated by the contribution of charged pions. In the intermediate x range, $x_{cr} < x < x_{cr}^K$, multiple pion scattering on photons becomes effective and therefore neutrinos from kaon decays start to provide the most important contribution to the total neutrino yield. Going to even higher energies, $x > x_{cr}^K$, leads to a strong suppression of neutrino from these decays as both pions and kaons most often scatter before decaying. Hence at high energies, neutrinos from decays of charm mesons represent the main component of the total neutrino yield. Moreover, the maximum of the neutrino yield does not coincide with that of the transparent cases, because τ is no longer proportional to the interaction depth.

In the bottom panel of Fig. 3, we show again neutrino yields but for a source with $T = 10^5$ K. If multiple scattering can be neglected, the neutrino yields are as expected independent from T and L . For $\tau > 1$, we observe the same behavior of the neutrino yields from pion and kaon decays as in the upper panel, but the suppression of their fluxes starts already at lower energies. As anticipated in the discussion of Fig. 1, the range of energies where neutrino fluxes are unsuppressed strongly depends on the energy threshold x_{th} and the critical energy x_{cr} . So, whereas for a source at $T = 10^4$ K the plateau visible in Fig. 3 for Y_{π} extends approximately over four orders of magnitude, in the case of a source at $T = 10^5$ K it is reduced by two orders of magnitude.

Finally, we want to illustrate how the high-energy suppression of neutrino fluxes depends on the interaction depth τ , as well as on the density and the typical energy of photons. Figure 4 shows (unnormalized) fluxes for a source at $T = 10^5$ K and different interaction depths, from 0.4 to 4×10^3 . In the case of thin sources, $\tau < 1$, we observe that the neutral proton flux is only slightly distorted relative to the initial flux, and therefore provides a non-negligible contribution to the observed UHE-CRs. The neutrino flux in these sources is basically proportional to the depth. For opaque sources the neutral proton flux becomes strongly suppressed above threshold, $E_p^{th} = m_p m = (2 \text{ GeV})$. For such high depths most pions and kaons scatter before decaying and as a consequence the flux of neutrinos becomes also suppressed at energies higher than E_{cr} . The only effect of further increasing τ is an increase of the low energy neutrinos, as the high number of scatterings leads to more low energy mesons. Figure 5 shows (unnormalized) fluxes for

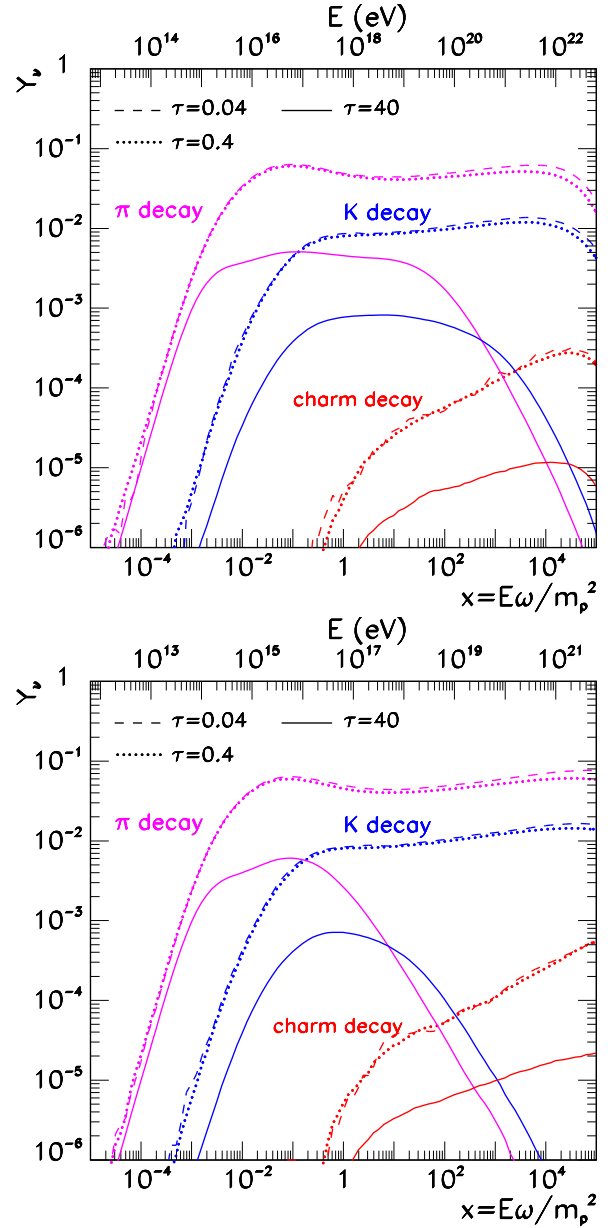


FIG. 3: Neutrino yield Y as function of $x = E \omega / m_p^2$ (bottom axis) and E (upper axis) from pion (magenta), kaon (blue), and charm decays (red) for $\tau = 0.04; 0.4$ and 40 ; upper panel for $T = 10^4$ K, lower panel for $T = 10^5$ K.

an opaque source, $\tau = 40$, at $T = 10^4$ K in the top and $T = 10^7$ K in the bottom. As previously mentioned, the neutral proton flux is strongly suppressed above threshold, whereas the neutrino flux rises already at lower energies, because they carry away only a fraction of the proton energy. The energy range where the neutrino flux is maximal extends approximately from E_p^{th} to E_{cr} , which for the source at $T = 10^4$ K, goes roughly from 10^{16} eV to 10^{20} eV. This range is strongly reduced for increasing T as $E_{cr} / 1 = n / 1 = T^3$, whereas $E_{th} / 1 = T$. Therefore, critical and threshold energies merge and only a nar-

low energy range around $E \sim 10^{12}$ eV with unsuppressed neutrino flux remains for $T = 10^7$ K, cf. the lower panel of Fig. 5.

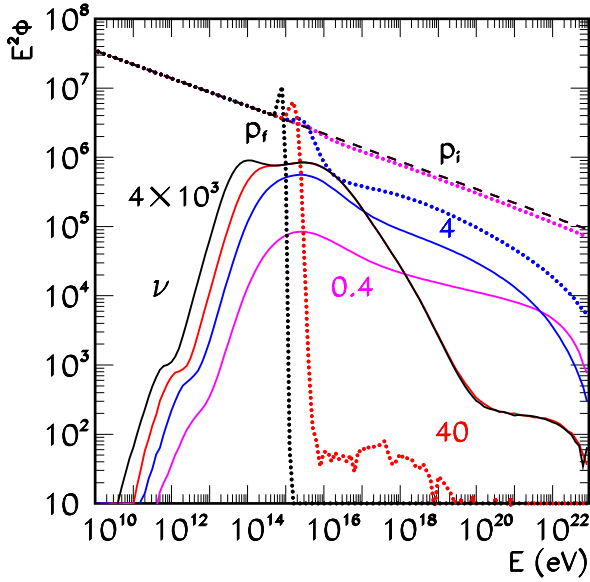


FIG. 4: Unnormalized fluxes of initial (dashed) and final (dotted) protons, as well as the total neutrino (solid), for a source at $T = 10^5$ K and with interaction depths $\tau = 0.4$ (magenta), 4 (blue), 40 (red) and 4×10^3 (black).

III. FLAVOR DEPENDENCE OF NEUTRINO YIELDS

Both neutrino telescopes and extensive air shower experiments have some flavor discrimination possibilities. The case of neutrino telescopes is discussed for the example of ICECUBE in detail in Ref. [15]. The long range of muons ensures that a muon track from charged-current interactions is always visible allowing the identification of these events. By contrast, the charged-current interactions of e and τ are as long as the tau decay length is too short to be detectable only distinguishable by the different muon content in electromagnetic and hadronic showers. Therefore, these two flavors are in practice impossible to differentiate for $E < 5 \times 10^4$ eV at a neutrino telescope. In the energy range $5 \times 10^4 \text{ eV} < E < 2 \times 10^6 \text{ eV}$, the “double-bang” signature [16] of τ gives some handle for the identification of this flavor, while for higher energies at least one of the two shower is outside a 1 km^3 detector. On the other hand, extensive air shower experiments have the potential to identify double-bang events in the small energy interval $5 \times 10^7 \text{ eV} < E < 2 \times 10^8 \text{ eV}$ [17]. In summary, the main observable for the neutrino flavor composition is the ratio of track to shower events in a neutrino telescope, $R = \nu_e / (\nu_e + \nu_\mu)$, while only in a very small

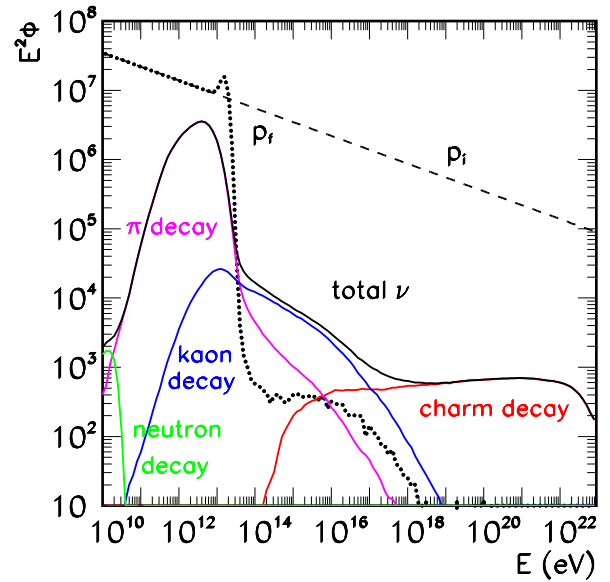
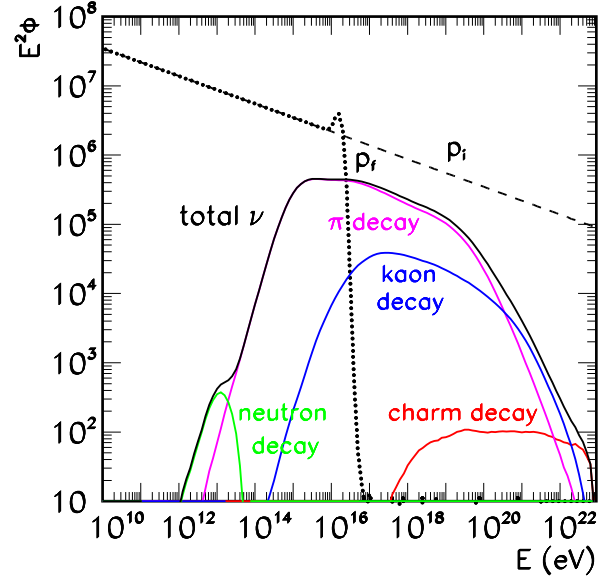


FIG. 5: Unnormalized fluxes of initial (dashed) and final (dotted) protons, as well as the total neutrino (solid), for a source with interaction depth $\tau = 40$ at $T = 10^7$ K (top) and $T = 10^5$ K (bottom). The different contributions to the total neutrino flux are also shown.

energy range all flavors can be distinguished. Additionally, extensive air shower experiments are sensitive to the fraction of tau events in all horizontal neutrino events, $R = \nu_\tau / (\nu_e + \nu_\mu)$, in a small energy window around 10^{18} eV.

In spite of these flavor discrimination possibilities, the potential of high energy neutrino observations for mixing parameter studies are only rarely discussed (for some recent examples see Ref. [18, 19]). One reason for this is the small number of events expected in next

generation experiments like ICECUBE or AUGER even in optimistic scenarios. Moreover, the neutrino flavor ratio from pion decay is $(\nu_e) : (\nu_\mu) : (\nu_\tau) = 1 : 2 : 0$ before oscillations, resulting into $(\nu_e) : (\nu_\mu) : (\nu_\tau) = 1 : 1 : 1$ at the detector quite independent from unknown details of the neutrino mixing matrix. Thus the maximum μ - τ mixing together with the initial flavor ratio $(\nu_e) : (\nu_\mu) : (\nu_\tau) = 1 : 2 : 0$ seems to disfavor high energy neutrino experiments as tools to probe only poorly known parameter θ_{13} or completely unknown ones as the octant of θ_{23} or the CP-violating phase δ_{CP} of the neutrino mixing matrix. As discussed in Refs. [18, 19], there exist however several examples of neutrino sources where at least in some energy range significant deviations from this canonical flavor ratio can be expected. Such a deviation does not only contain information about neutrino properties but also their sources. For instance, Ref. [20] discussed the possibility to distinguish between pp or p sources of neutrinos measuring their flavor ratios. In the following, we will show that opaque sources are characterized by an energy-dependent flavor ratio and thus the flavor ratio encodes non-trivial information.

A. Energy dependence of the neutrino flavor ratio at the source

We start with an analysis of the expected neutrino flavor ratio $R^0 = Y_\nu / Y_e$ at the source. In Fig. 6, we show R^0 separately for each reaction contributing to the neutrino yield in the case of a source with $T = 10^4$ K. For definiteness we have set $R^0 = 0$, if $\chi(x) = \nu_p(E) < 10^{-6}$. The two panels show R^0 for transparent source with interaction depth $\tau = 0.04$ (top) and $\tau = 40$ (bottom), respectively.

In pion decays, all three neutrinos produced have very similar energy spectra and therefore R^0 is close to two. The most important decay channel of charged kaons is the same as the one of charged pions, $K^+ \rightarrow \pi^+ \ell^+ \nu_\ell$, $2 \rightarrow e + e$. However, the mass difference between kaons and muons leads to very different energy distributions of the directly produced neutrinos. The neutrino spectra from kaons are dominated at low energies by neutrinos from muon decay, whereas at high energies ν_μ 's produced in the direct kaon decays dominate. As a consequence, there are three different ranges for the flavor ratio R^0 of neutrinos produced by the charged kaon decays: At low energies the contribution of the direct ν_μ is negligible. Thus R^0 approaches one at low energies, since the ν_e and ν_μ spectra from muon decay are similar. Near the threshold energy for kaon production, $x_{th}^K \approx 0.2$, direct ν_μ 's start to dominate, leading to an increase of R^0 to values larger than two. The particular value of R^0 within this energy range depends on the initial kaon spectrum: the steeper it is, the larger the flavor ratio. As the energy increases the neutrino flavor ratio remains roughly constant until it gets closer to the high energy kinematical limit. At this point there are practically only ν_μ 's from

the direct kaon decay and therefore R^0 increases fast. In the case of neutrinos produced in neutral kaon decays one expects a flavor ratio between two, corresponding to the contribution from K_S^0 (via $K_S^0 \rightarrow 2\pi$), and roughly one, due to the neutrino yield from the K_L^0 decay, mainly from $K_L^0 \rightarrow \pi^+ \ell^+ \nu_\ell$. Finally, concerning the neutrinos generated in the decay of charm mesons one observes the same contribution from ν_e and ν_μ , leading to a flavor ratio of one [23].

The flavor ratio for an opaque source with $\tau = 40$ (bottom panel) is only changed for neutrinos from kaon decays. At energies larger than x_{cr}^K most of charged kaons scatter before decaying, leading to a steeper spectrum of the kaons which eventually decay. As a consequence at that point the value of R^0 increases a second time before approaching the high energy limit. Roughly at the same energies the pions emitted by K_L^0 scatter before decaying. Therefore, in contrast to transparent sources, the flavor content of K_L^0 's at high energies is dominated by ν_e and the ratio R^0 tends to values smaller than one.

Let us now consider the total flavor ratio expected for different sources, shown in the Fig. 7. In the case of a transparent source the value of R^0 is small at low x because almost all neutrinos are produced in the decay of neutrons, see Fig. 2. Once the contribution from charged pion decay becomes dominating, R^0 approaches the standard value two, as expected from the upper panel of Fig. 6. In contrast to transparent sources, in the case of an opaque source, $\tau = 40$, R^0 is strongly energy-dependent. In particular, the flavor ratio reaches the value of 2 at lower x , because multiple scattering of nucleons leads to lower energies of the escaping neutrons. Moreover, there is a bump in the range $100 < x < 10^4$ and $1 < x < 100$ for the case $T = 10^4$ K and 10^5 K, respectively. The lower limit of these ranges corresponds to the cross-over between pion and kaon dominance, while the upper limit corresponds to the cross-over between kaon and charm dominance. As can be inferred from the right panel of Fig. 6, the value of R^0 at the bump is determined by the interplay of the charged and neutral kaon neutrinos. Finally, in both cases the asymptotic value is $R^0 = 1$, which corresponds to the ratio expected when the decay of charm mesons dominates.

B. Effect of neutrino oscillations

The neutrino spectra at the source discussed in the preceding subsection are modulated by oscillations. Therefore the expected flavor ratios R_i at the Earth are different from the original ratios R_i^0 at the source.

The neutrino fluxes arriving at the detector, Φ^D , can be written in terms of the initial fluxes Φ^S and the conversion probabilities P_{ij} ,

$$\Phi^D = \sum_i P_{ij} \Phi^S_j = P_{ee} \Phi_e + P_{\mu e} \Phi_\mu + \dots \quad (3)$$

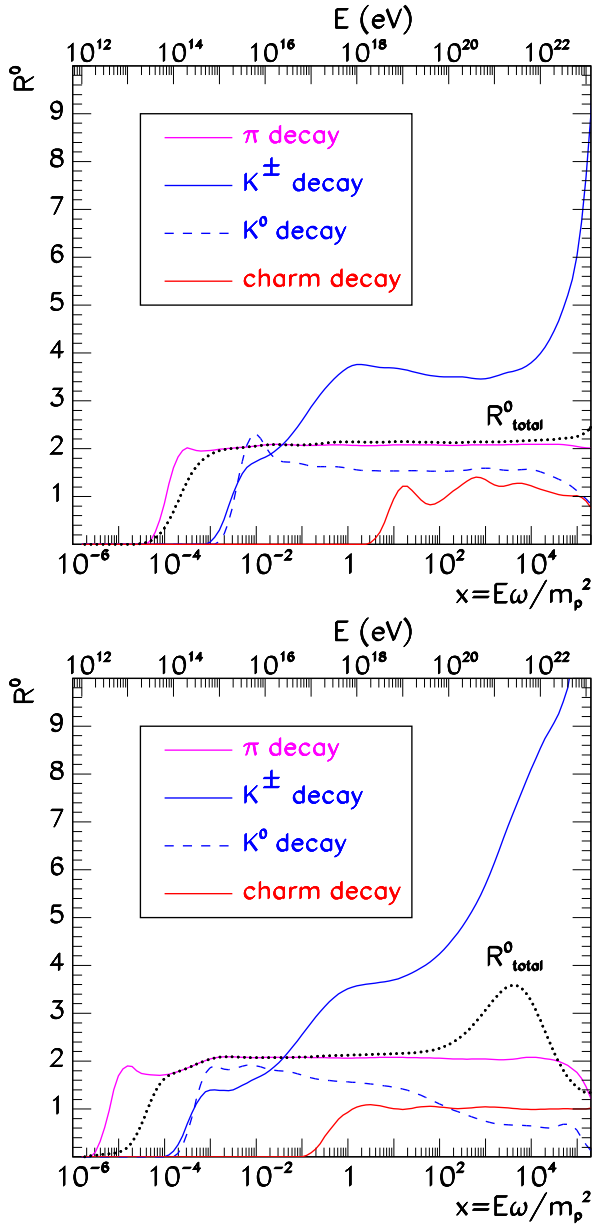


FIG. 6: Flavor ratio R^0 of the neutrinos produced in a source before they oscillate in terms of $x = E\omega/m_p^2$. Top: Specific flavor ratio for the neutrinos generated from the decay of π (magenta), K^\pm (solid blue), K^0 (dashed blue), and charm meson (red) for a source with $T = 10^4$ K and $\tau = 0.04$. In black dotted line is shown the total R^0 . Bottom: The same for a source with interaction depth $\tau = 40$.

Since the interference terms sensitive to the mass splittings m^2 's do not contribute, the conversion probabilities are simply

$$P_{jk} = \frac{1}{2} \sum_{l>k} \langle (U_{jl}^* U_{kl} U_{jl} U_{kl}^*) \rangle; \quad (4)$$

where U is the neutrino mixing matrix and Greek (Latin) letters are used as flavor (mass) indices. In Fig. 8, we

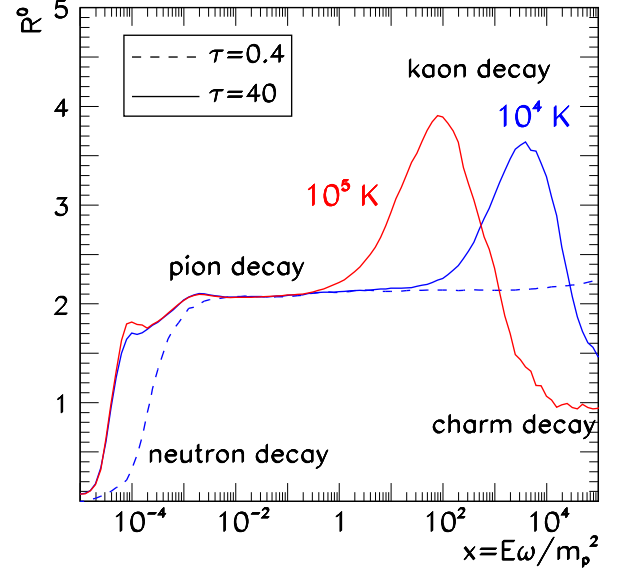


FIG. 7: Total flavor ratio for a source at $T = 10^4$ K and $\tau = 0.4$ (blue dashed), $T = 10^4$ K and $\tau = 40$ (blue solid), and $T = 10^5$ K and $\tau = 40$ (solid red). The main reactions giving rise to the neutrino signal are also shown.

show the expected flavor ratio R at the detector in the case of a source with $T = 10^5$ K and $\tau = 40$ as a solid, red line for the best-fit point of the neutrino mixing parameters, $\sin^2 \theta_{12} = 0.3$; $\sin^2 \theta_{23} = 0.5$ and $\theta_{13} = 0$ [21]. Various bands show the range of R allowed if the mixing parameters are varied within their 95% C.L., while the unconstrained CP phase δ_{CP} is varied in the whole possible range, $\delta_{CP} \in [0, 2\pi]$. Dominant uncertainty for the prediction of R is the value of θ_{23} .

We analyze next the dependence of the flavor ratio R on the different neutrino mixing parameters in more detail. Expanding R up to first order in θ_{13} and choosing for illustration $\theta_{12} = \theta_{23} = 6$ gives

$$R(R^0; \theta_{23}; \theta_{13}; \delta_{CP}) = \frac{P_{ee} + R_0 P}{P_{ee} + R_0 P_e + P_e + R_0 P} = A(R^0; \theta_{23}) + B(R^0; \theta_{23}) \cos \delta_{CP} \theta_{13} + O(\theta_{13}^2); \quad (5)$$

The explicit expression for A and B are given in the Appendix. In Fig. 9, we show the dependence of the coefficients A (left panel) and B (right panel) on R^0 and θ_{23} . While the parameter A is more sensitive to the value of R^0 if θ_{23} is in the second octant, $\sin^2 \theta_{23} > 0.5$, this behavior is opposite for B .

Let us first analyze the dependence of R on θ_{23} . For the sake of simplicity, we assume $\theta_{13} = 0$, and thus $R(R^0; \theta_{23}; 0; \delta_{CP}) = A(R^0; \theta_{23})$. The upper panel of Fig. 10 shows the flavor ratio R for different values of $\sin^2 \theta_{23}$. The possibility to extract information about the value of θ_{23} strongly depends on the energy range considered. At low energies, where the initial ra-

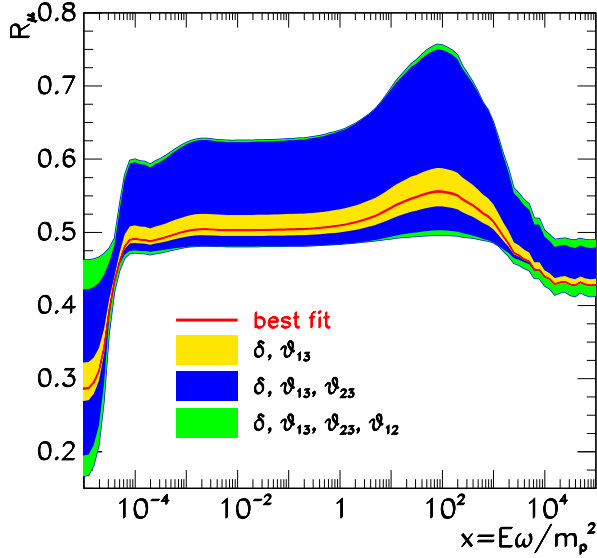


FIG. 8: Flavor ratio R_μ at the Earth for a source with $T = 10^5$ K and $\theta = 40^\circ$. The solid red line corresponds to the best fit point of the neutrino mixing parameters, $\sin^2 \theta_{12} = 0.3$, $\sin^2 \theta_{23} = 0.5$ and $\theta_{13} = 0$. In the colored areas mixing angles within 95% C.L. and a possible non-zero value of θ_{CP} have been considered: θ_{13} and θ_{CP} (yellow), plus θ_{23} (blue), and θ_{12} (green).

ratio is close to zero (neutron neutrinos), R_μ depends inversely on $\sin^2 \theta_{23}$, varying between 0.15 and 0.35 for $\sin^2 \theta_{23} = 0.65$ and 0.35 , respectively. This large sensitivity of R_μ to the value of θ_{23} makes the neutrinos emitted in neutron decay an alternative tool to study this mixing angle [19]. At intermediate energies the sensitivity becomes smaller. When neutrinos come mainly from charged pion decays, $R^0 \approx 2$, we observe basically two regions: below $\sin^2 \theta_{23} \approx 0.52$, the flavor ratio at the Earth lies around 0.5, whereas for larger angles it grows until values around 0.6. This is a consequence of the different behavior of A at R^0 larger than one for θ_{23} in the first octant, see the upper panel of Fig. 9. This difference can even increase at the bump, where R_μ can reach values larger than 0.7 for θ_{23} in the second octant whereas it remains smaller than 0.6 for angles in the first octant. Finally at higher energies (charm neutrinos) it becomes very difficult to disentangle the different values: $R^0 \approx 1$ and R_μ becomes roughly 0.45 for all θ_{23} around $\theta = 4^\circ$, see upper panel of Fig. 9.

Let us now briefly discuss the dependence of R_μ on θ_{13} and θ_{CP} . According to Eq. (5), this variation depends on R^0 and θ_{23} through the function $B(R^0; \theta_{23})$. The bottom panel of Fig. 9 shows that the maximal variation takes place when θ_{23} is in the first octant and R^0 deviates significantly from one. In all cases, though, the sensitivity does not exceed 10%. In the bottom panel of Fig. 10, we show the variation of R_μ for values of θ_{13} between 0

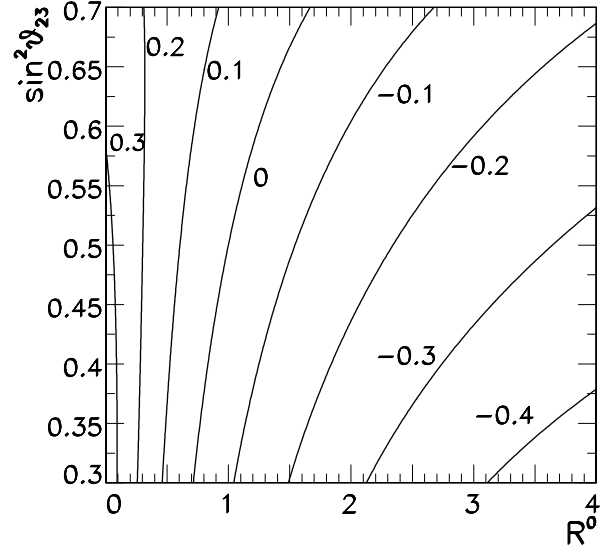
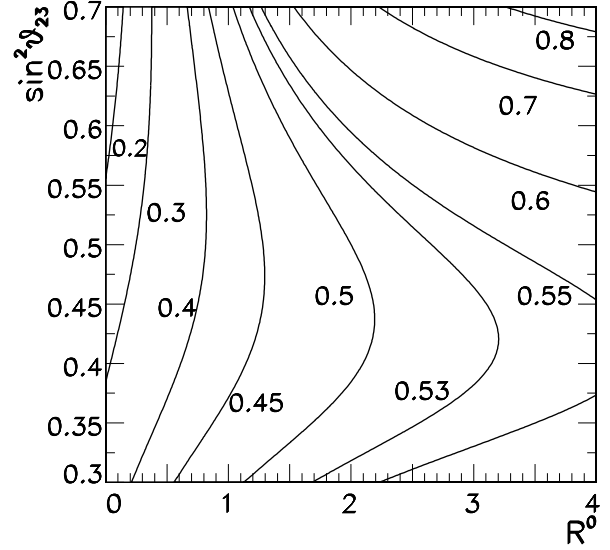


FIG. 9: Contours of the coefficients $A(R^0; \theta_{23})$ (top) and $B(R^0; \theta_{23})$ (bottom) in terms of R^0 and $\sin^2 \theta_{23}$.

and 10° , assuming $\theta_{CP} = 0$ and $\sin^2 \theta_{23} = 0.35$ (green) and 0.65 (yellow). While at low energies ($R^0 \approx 0$) both cases give similar results, at higher R^0 the dependence on θ_{13} is almost negligible. We show also the variation of R_μ as function of θ_{CP} for the same values of $\sin^2 \theta_{23}$ and $\sin^2 \theta_{13} = 10^{-2}$. In this case, the variation is larger due to the two different signs of $\cos \theta_{CP}$.

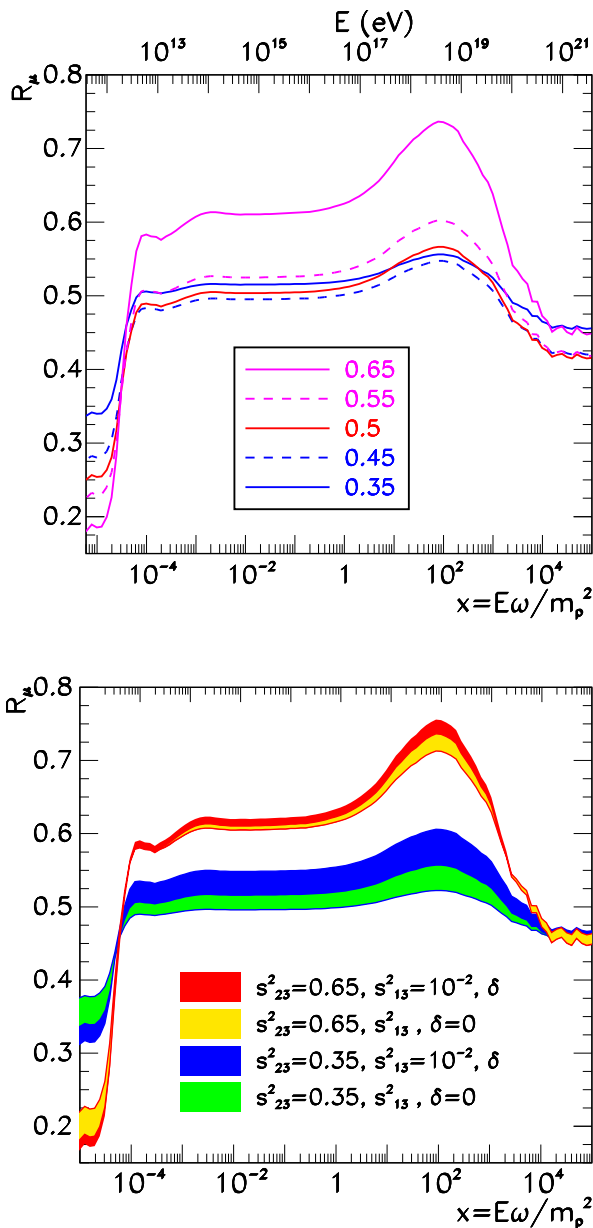


FIG. 10: Top: Flavor ratio at the Earth R^α for different values of $\sin^2 \theta_{23}$ assuming $\sin^2 \theta_{12} = \approx 6$ and $\theta_{13} = 0$ for a source at $T = 10^5$ K and interaction depth $\tau = 40$. Bottom: Dependence of R^α on θ_{13} for $\theta_{CP} = 0$ (yellow and green), and on θ_{CP} , assuming $\sin^2 \theta_{13} = 10^{-2}$ (red and blue), for two extreme values of $\sin^2 \theta_{23}$.

IV. SUMMARY

The high-energy cosmic ray flux from opaque or hidden neutrino sources is suppressed and these sources are there-

fore among the most promising candidates for powerful neutrino sources. We have calculated the yield of high energy neutrinos from sources with photons as target material, paying especially attention to opaque sources. We have found that the neutrino spectra from meson and muon decays are strongly modified with respect to transparent sources as soon as multiple scattering of nucleons becomes important. The main consequence is a strong suppression of the neutrino flux from pion and kaon decays at energies above a critical energy E_{cr} , defined as the energy at which the scattering length of mesons equals the decay length. Above this energy both pions and kaons scatter before decay and thus the main contribution to the neutrino flux is supplied by the decay of charm mesons. As a result, the parameter range where opaque sources can produce ultra-high energy neutrinos is rather restricted. An opaque source with $E_{cr} > 10^{21}$ eV requires basically a large extension with low densities.

Both neutrino telescopes and extensive air shower experiments can not only detect high energy neutrinos but also they have some flavor discrimination possibilities. Since the determination of the neutrino flavor ratio can shed light on the properties of both sources and neutrinos, we have calculated also the expected flavor ratio for opaque sources containing photons as scattering targets. The main characteristic is a strong energy-dependence of the ratio R^α of ν_e and ν_μ fluxes at the sources. A generic prediction for neutrinos from hadron-photon scattering is the flavor ratio $R^\alpha \approx 0$ below the threshold, i.e. a flux dominated by ν_e at the source. In the case of opaque sources the flavor ratio presents a bump close to the energy where the decay length of charged pions and kaons equals their interaction length on target photons. The neutrino spectra at the source are modulated by oscillation. Therefore the expected flavor ratio R^α at the Earth will be different from the original one R^α : it significantly depends on the neutrino mixing parameters, and especially on θ_{23} . Therefore the observation of a strong energy dependence of R^α will not only be a hint on the kind of source but also allow obtaining complementary information on the neutrino mixing angles.

Acknowledgments

We would like to thank Pedro Ruiz-Femenia and in particular Sergey Ostapchenko for useful and pleasant discussions. RT was supported by the Juan de la Cierva programme, an ERG from the European and by the Spanish grant FPA 2005-01269. We would also like to thank the European Network of Theoretical Astroparticle Physics ILIAS/N 6 under contract number R IIB-CT-2004-506222.

APPENDIX : T W O T W O - C O L U M N F O R M U L A E

The explicit expression for A and B are

$$A(R^0; \theta_{23}) = \frac{12 + 39R^0 \cos(2\theta_{23}) + 13R^0 \cos(4\theta_{23})}{52 + 25R^0 + 12(R^0 \cos(2\theta_{23}) + 13R^0 \cos(4\theta_{23}))} \quad (6)$$

$$B(R^0; \theta_{23}) = \frac{512 \sqrt{3} (1 + R^0) (1 + R^0 + R^0 \cos(2\theta_{23})) \sin(2\theta_{23})}{[52 + 25R^0 + 12(R^0 \cos(2\theta_{23}) + 13R^0 \cos(4\theta_{23}))]^2} \quad (7)$$

-
- [1] V. Berezinsky, Nucl. Phys. Proc. Suppl. 151, 260 (2006) [astro-ph/0505220]; P. Lipari, astro-ph/0605535.
- [2] V. S. Berezinsky and G. T. Zatsepin, Phys. Lett. B 28, 423 (1969), Sov. J. Nucl. Phys. 11, 111 (1970); for a recent works see e.g. D. V. Semakoz and G. Sigl, JCAP 0404, 003 (2004) [hep-ph/0309328].
- [3] V. S. Berezinsky and A. Yu. Smirnov, Astrophys. Space Sci. 32, 461 (1975); V. S. Berezinsky, in Proc. of "Neutrino-77", Baksan, USSR, ed. M. A. Markov 1, 177 (1977).
- [4] E. Waxman and J. N. Bahcall, Phys. Rev. D 59, 023002 (1999) [hep-ph/9807282].
- [5] K. Mannheim, R. J. Protheroe and J. P. Rachen, Phys. Rev. D 63, 023003 (2001) [astro-ph/9812398].
- [6] B. Eberle, A. Ringwald, L. Song and T. J. Weiler, Phys. Rev. D 70, 023007 (2004) [hep-ph/0401203].
- [7] V. Berezinsky and V. V. Volynsky, Proc. 17th Int. Cosmic Ray Conf., vol. 10, p. 326; *ibid* p. 332, *ibid* p. 338 (Kyoto, 1979).
- [8] V. S. Berezinsky and A. Z. Gazizov, Phys. Rev. D 47, 4206 (1993); *ibid*. 47, 4217 (1993).
- [9] J. P. Rachen and P. Meszaros, Phys. Rev. D 58, 123005 (1998) [astro-ph/9802280].
- [10] A. Mücke et al., Comput. Phys. Commun. 124, 290 (2000) [astro-ph/9903478].
- [11] G. Corcella et al., JHEP 0101, 010 (2001) [hep-ph/0011363].
- [12] A. V. Berezhnoy, V. V. Kisilev and A. K. Likhoded, Phys. Rev. D 62, 074013 (2000).
- [13] An improved treatment of meson-gamma interactions is in preparation, cf. Ref. [14].
- [14] M. Kachelrieß, S. Ostapchenko and R. Tomas, High energy neutrino yields from astrophysical sources II: General case, in preparation.
- [15] J. F. Beacom et al., Phys. Rev. D 68, 093005 (2003) [Erratum-*ibid*. D 72, 019901 (2005)] [hep-ph/0307025].
- [16] J. G. Learned and S. Pakvasa, Astropart. Phys. 3, 267 (1995) [hep-ph/9405296].
- [17] H. Athar, G. Parente and E. Zas, Phys. Rev. D 62, 093010 (2000) [hep-ph/0006123]; H. Athar, hep-ph/0004083.
- [18] P. Bhattacharjee and N. Gupta, hep-ph/0501191; T. Kashti and E. Waxman, Phys. Rev. Lett. 95, 181101 (2005) [astro-ph/0507599]; P. D. Serpico and M. Kachelrieß, Phys. Rev. Lett. 94, 211102 (2005) [hep-ph/0502088]; W. Winter, hep-ph/0604191.
- [19] P. D. Serpico, Phys. Rev. D 73, 047301 (2006) [hep-ph/0511313].
- [20] L. A. Anchordoqui, H. Goldberg, F. Halzen and T. J. Weiler, Phys. Lett. B 621, 18 (2005) [hep-ph/0410003].
- [21] M. Maltoni, T. Schwetz, M. A. Tortola and J. W. F. Valle, New J. Phys. 6, 122 (2004) [hep-ph/0405172].
- [22] Throughout the present work we will not distinguish neutrinos from antineutrinos. Therefore ν will represent the sum of $\nu + \bar{\nu}$.
- [23] The production is negligible in comparison to the other flavors.